Numerical Analysis of LBV150 ROV Thruster Performance Under Open Water Test Condition

Ngo Khanh Hieu[(✉)], Phan Quoc Thien, and Nguyen Ho Nghia

Ho Chi Minh City University of Technology (HCMUT),
Ho Chi Minh City, Vietnam
ngokhanhhieu@hcmut.edu.vn, phanquocthien@gmail.com,
nhnghia208@gmail.com

Abstract. Remotely operated vehicles (ROVs) research has increased remarkably because of the technological improvements in ROV's. The LBV150 ROV is a highly-maneuverable miniROV of the SeaBotix Incorporation serving a range of military, commercial, and scientific, which uses HPDC 1507 thrusters for the propulsion system. In this article, the simulation for the LBV150 ROV thruster performance during forward mode under open water test condition is developed together with OpenFOAM. The static thrust coefficient of the thruster obtained from the simulation is validated by the acceptance testing of this thruster in the open water channel at HCMUT. So, the other characteristics of the thruster performance including thrust coefficient, power coefficient, efficiency, pressure distribution as well as velocity of flow around the thruster, etc. could be produced as the result of the simulation. The proposed numerical analysis could help to develop a simulation tool for the design of miniROV propulsion system.

Keywords: ROV's thruster performance · Numerical analysis with OpenFOAM · ROV's thruster testing system

1 Introduction

A remotely operated vehicle (ROV) is a tethered underwater mobile device. This meaning is different from remote control vehicles operating on land or in the air. ROVs are unoccupied, highly maneuverable, and operated by a crew aboard a vessel. ROV is a safe and widely used type of underwater vehicle serving a range of military, commercial, and scientific requirements [1]. These requirements can perform with a variety of methods, such as calculating by theory, simulation and experimentation. In these methods, the experimental method has the highest accuracy, but it takes more time and costs. However, the development of computer science with the mainframe system can process fast and accuracy along with the development of different simulation tools as OpenFOAM, ANSYS, MOLEX3D… Hence, the computational fluid dynamic (CFD) has become the most common method because of its less time and lower cost than the experimental approach.

CFD is one of the most popular numerical approaches for predicting the external flow around different kinds of vehicles and analyzing the internal flow through many

types of tube or duct. All of the CFD methods are based on the fundamental governing equations of fluid dynamics, such as the continuity, momentum, and energy equations which are the mathematical statements of three physical principles: Law of Mass Conservation, Newton's Second Law, and Law of Energy Conservation. However, our model is incompressible fluid that does not require energy equation [2]. The turbulence model is one of the most popular models and it is widely used in CFD. It is used to predict the effects of turbulence in the fluid flow without resolving all scales of the smallest turbulent fluctuations based on the Navier-Stokes equations [3]. The k-ε model improves the robustness; the accuracy and the result for the near-wall mesh are precise because the scalable wall-function approach is applied. It ensures the stability when solving the problem.

In the Aerospace Engineering Department at HCMUT, the use of CFD is quite frequent as a wind tunnel simulation tool during the preliminary design of aircraft of the following analysis of aerodynamic coefficients [4, 5]. To simulate the rotating surfaces, the common methods are moving mesh, Multi-Reference Frame (MRF) or Single Reference Frame (SRF). Moving mesh is the method in which the mesh interfaces between the rotating region containing rotating surface and the static region slide into each other and is assigned as cyclic boundaries. Moving mesh is normally used in unsteady state solver and highly time consuming comparing to SRF and MRF which are implemented in steady state solver. MRF is the method in which the mesh for the simulation domain is separated into two different regions. They are rotating region containing rotating surface and static region covering the rest of the domain like mesh for moving mesh method, however, there is no moving parts as well as cyclic boundaries in the mesh. Thereby, in the rotating region of MRF method, a mathematical term is added into momentum equations to model the rotating effect and a different reference coordinate system is applied. In term of reference system, SRF method is simpler than MRF method since cylindrical coordinate system with the longitudinal axis is rotating axis of moving surface is applied not only for rotating region like MRF but also for the whole domain. That means, in SRF method, the whole domain is rotating region. Consequently, SRF method is relatively unstable, especially when the domain is large and rotation is in high revolution, because the reference velocity is high correspondingly [6, 7]. Therefore, in this research, MRF method along with steady state solver is the selected to estimate the behavior of the LBV150 ROV.

The LBV150 ROV is a highly maneuverable miniROV of SeaBotix Incorporation serving a range of military, commercial, and scientific, which uses HPDC 1507 thrusters for the propulsion system (see Fig. 1). In this article, a simulation of the dynamics of the SeaBotix LBV150 ROV thruster during forward mode under open water condition based on OpenFOAM will be developed. Because the Reynolds number of our model is high, the water flow over the propeller blades will be fully developed turbulence. The standard k-ε model is chosen to estimate turbulent effect in this simulation due to its compatibility for wide range of flow patterns with long history of benchmarking, less computational intense as well as less requirement of refining boundary layer compared to other turbulent models for high Reynold number which is varying from 1.9×10^5 to 2.4×10^5 within this study. The static thrust coefficient of the thruster obtained from the simulation will be validated by the acceptance testing of this thrusters in the open water tunnel at HCMUT. So the other characteristics of the

LBV150 ROV thruster performance including thrust coefficient, power coefficient, efficiency, pressure distribution of flow around the thruster, etc. could be produced as the result of the simulation.

Fig. 1. The SeaBotix LBV150 ROV and its thruster

In the next section, the SeaBotix LBV150 ROV thruster's thrust test-rig will be presented, and the experimental results is used to validate the simulation of this thruster's static thrust.
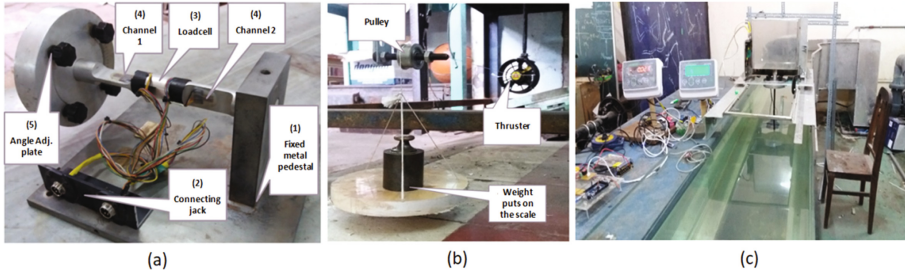
2   LBV150 ROV Thruster's Thrust Test-Rig

The main purpose of this section is to design a thrust testing for the LBV150 ROV thruster. The test-rig can be integrated into the open water tunnel with the test section of $2.0 \times 0.5 \times 0.5$ m (length $\times$ depth $\times$ width) in the Naval Architecture and Marine Engineering Lab. at HCMUT. Figure 2a shows the balance used for thruster thrust testing. It is a two-channel-balance based on the strain gauge, which could measure forces in two perpendicular directions (corresponding to the forward force and the side-force of the thruster) and could be adjusted by an angle adjustable plate. A mount is designed to fix the balance vertically to the test section of the water tunnel (see Fig. 2c).

The calibration with the standard weights is shown in Fig. 2b. The relationship between the weights and the values obtained by this balance is linear with a correlation coefficient of $0.9999 \div 1.0000$. It means that the proposed thrust test-rig could be used for thrust testing of the LBV150 ROV thruster.

After many experiments were conducted, the following graphs indicate the static thrust characteristics of the LBV150 ROV thruster during forward mode. The results from HCMUT is compared with the datasheet of the SeaBotix [8]. The HCMUT results in forward mode have the maximum error of 10.7% (see Fig. 3a). It's obviously very difficult to achieve the same experimental conditions as the manufacturer. Furthermore, the test section of the open water tunnel in HCMUT is also not large enough. The thruster's static thrust testing from HCMUT could achieve reasonable static thrust

coefficients (C_{To}) in order to validate the results obtained from the simulation (see Fig. 3b, noting that RPM is the rotational speed of thruster in revolutions per minute. And the C_{To} of SeaBotix is calculated by assuming that the relationship between the RPM and the voltage of the thruster is the same with the HCMUT thrust testing).

Fig. 2. LBV150 ROV thruster's thrust test-rig at HCMUT (a) 2 channels balance; (b) balance calibration; (c) testing system fixed on open water tunnel
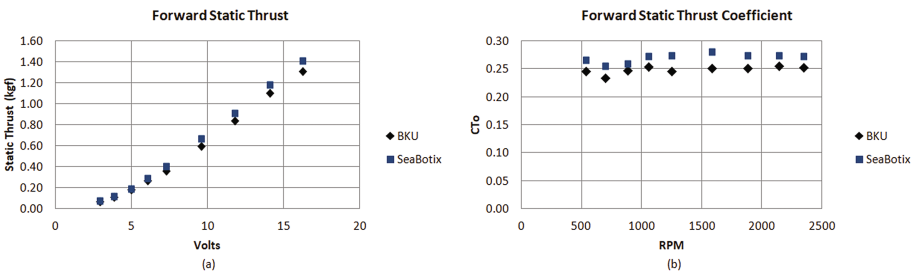
Fig. 3. LBV150 ROV thruster's static thrust characteristics using the HCMUT test-rig (a) Static thrust vs. volts; (b) static thrust coefficient vs. RPM

3   3D Modeling of the LBV150 ROV Thruster

The 3D model of the Seabotix LBV150 ROV thruster is created by a 3D scanning method (see Fig. 4). Table 1 shows the primary parameters of this thruster obtained from its 3D model. The geometry error between the 3D model and the actual thruster [8] is up to 1%.

Fig. 4. 3D model of the LBV150 ROV thruster

Table 1. Primary geometrical parameters of LBV150 ROV thruster

| Propeller diameter (D)	76.0 mm
Inner diameter of duct	79.0 mm
Outer diameter of duct (D_{duct})	94.6 mm
Number of propeller blade	02
Diameter of pod housing	44.0 mm
Overall length of thruster	174.5 mm

In the next sections, this 3D model is used for the simulation of the LBV150 ROV thruster performance.

4 Numerical Analysis of the SeaBotix LVB150 ROV Thruster

4.1 Mesh Generation for Simulation

Since the generation of hexahedral grid requires a lot of effort for meshing complex shapes like thruster geometry to achieve high quality elements, using tetrahedral mesh is an advantage. The tetrahedral mesh is easy to generate and can be automatically created, although there are more volume elements than the equivalent hexahedral mesh. This leads to the disadvantages of the high computing cost and instability as well as longer time of mathematical respond [9, 10, 12]. However, these drawbacks can be easily managed by high performance hardware and steady state solver combine with high order schemes. Therefore, tetrahedral mesh is proceeded within this work.

The mesh covers the domain limited by 7 separated boundary faces as Fig. 5 so that the dimensions of the domain are correlated to the outer diameter of the duct (Dduct) to reduce mathematical effects by boundary conditions. The free flow comes from inlet and exits the domain at outlet while inner surface of the duct bounds a sub-domain for rotating zone which is applied different frame of reference in Multiple Reference Frame Model (MRF) for steady rotating problem [11]. In the farfield boundary, the fluid flow is set to be zero gradient as it is considered not to be affected by the rotating part.
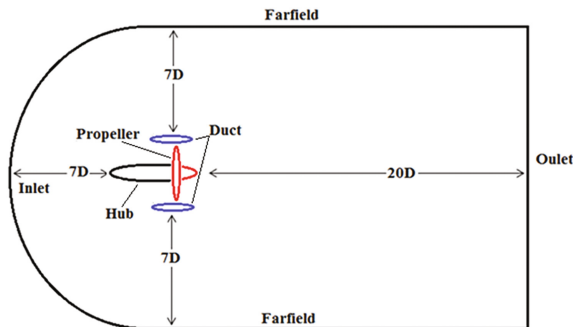
Fig. 5. Mesh domain for simulation of the LBV150 ROV thruster

The 5.2 million-cell mesh, which is composed of 4.7 million tetrahedral elements and 0.5 million triangular prisms, layers (see Fig. 6). Before running in OpenFOAM, this mesh was carefully checked and satisfied all OpenFOAM criteria. The maximum non-orthogonally is lower than 70 and also the max skewness is not over 2.5. In addition, for the wall boundaries of duct, propeller and hub, the thickness of the layers was estimated for the highest revolution in order to limit the value of Y+ in a suitable range when applying wall function.
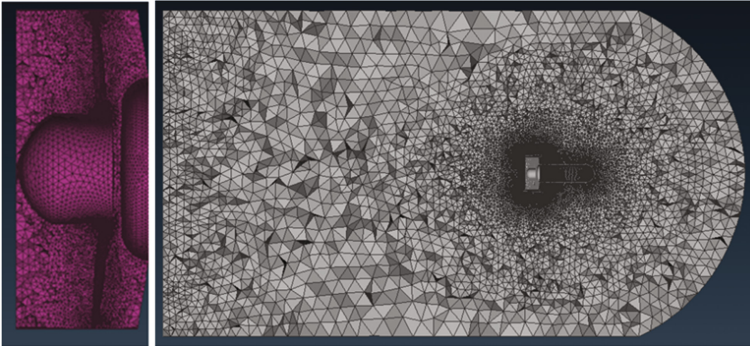
Fig. 6. LBV150 ROV thruster mesh with tetrahedral elements and triangular prism layers

## 4.2   Simulation of Dynamics of the SeaBotix LBV150 ROV Thruster

Firstly, the k-ε OpenFOAM solver is used to analyze the characteristics of the thruster in static conditions at different rotational speeds. So the rotation speed of the thruster is changed from 1300 RPM to 2500 RPM (which corresponds to the thruster's Reynolds number from 1.2×10^5 to 2.4×10^5). All equations use an under-relaxation factor of 0.7 except pressure correction that has a relaxation factor 0.3. The boundary conditions are presented in Table 2. The static thrust characteristics obtained by the simulation was compared with the HCMUT testing results (see Fig. 7). The Table 3 represents the thruster characteristics in static condition obtained by simulation.

Table 2. Boundary conditions for the simulation of LBV150 ROV thruster

The boundary	P	U	k	Epsilon
Blade/Duct/Tail	zeroGradient	fixedValue	kqRWallFunction	epsilonWallFunction
Farfield	fixedValue	inletOutlet	inletOutlet	inletOutlet
Inlet	zeroGradient	fixedValue	turbulentIntensity-KineticEnergyInlet	turbulentMixingLength-DissipationRateInlet
Outlet	fixedValue	inletOutlet	inletOutlet	inletOutlet

From the simulation, the static thrust coefficient of thruster is about 0.272. Meanwhile, the experimental results conducted at HCMUT testing have a static thrust

coefficient of 0.251 at RPM being from 1241–2342 RPM, therefore the error of thruster's static thrust coefficient between simulation and HCMUT testing is approximately 8.40%. The proposed numerical analysis could achieve reasonable characteristics of LBV150 ROV thruster performance during forward mode in static condition.
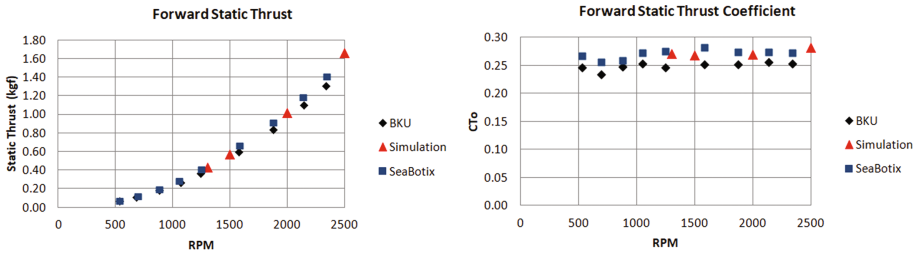
Fig. 7. Thrust characteristics of thruster in static condition: simulation results and HCMUT testing

Table 3. LBV150 ROV thruster characteristics in static condition

Simulation				HCMUT thrust testing		
RPM	Thrust (kg.f)	C_{To}	C_{Po}	RPM	Thrust (kg.f)	C_{To}
1300	0.433	0.271	0.204	1250	0.362	0.246
1500	0.569	0.267	0.200	1584	0.593	0.251
2000	1.016	0.268	0.198	2141	1.103	0.255
2500	1.665	0.282	0.204	2344	1.309	0.252
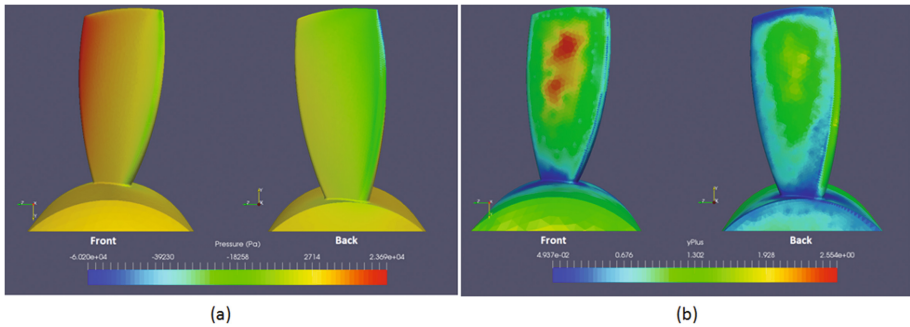
Fig. 8. Pressure distribution (a) and Y+ distribution (b) on propeller blades at 2000 RPM in static condition

Figure 8 represents the pressure and the Y+ distribution on propeller blades of the thruster at 2000 RPM, which corresponds to the thruster's Reynolds number of 1.9×10^5, in static condition.

Figure 9a represents the static power coefficient (CP_o) of the thruster obtained by the simulation. This power coefficient value is about 0.201. By following Andreas Johannes Häusler [13], the actual propeller power (P_a) can be determined from the rate motor power (P_N) at continuous operation and the mechanical efficiency (η_m). Where,

- $P_N = P_{max}/k_m = 100/1.1 = 90.91$ W (note that P_{max} corresponds to 100 W thruster; $k_m \in [1.1; 1.2]$ is the maximum motor torque/power constant).
- $P_a = \eta_m \times P_N = 54.54$ W (in industrial application, a constant mechanical efficiency $\eta_m \in [0.6; 0.7]$ is usually assumed).

As the result of the simulation, 100 W thruster could develop a normal forward mode in static condition at speed of 2848 RPM. So 100 W thruster could develop 2.08 kg.f forward static thrust. The datasheet of the SeaBotix LBV150 ROV thruster [8] indicates that 100 W thruster develops over 2.0 kg.f forward thrust.
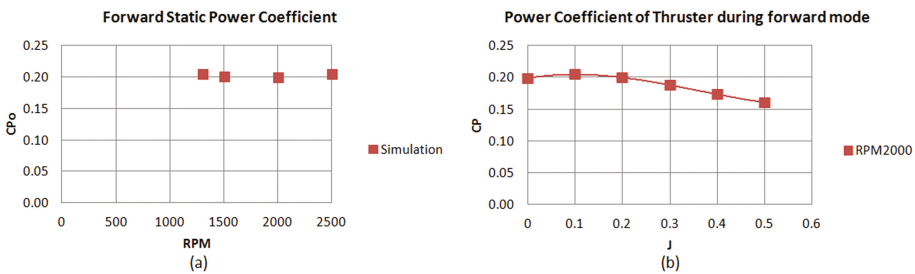

Fig. 9. Power coefficient of LBV150 ROV thruster during forward mode (a) at 2000 RPM in static condition; (b) at 2000 RPM vs. J

Finally, from the simulation of the performance of the Seabotix LBV150 ROV thruster during forward mode can be described in terms of the relationship between the dimensionless coefficients and the advance ratio (J). They are the thrust coefficient, C_T, (see Fig. 10a), the power coefficient, C_P, (see Fig. 9b) and the efficiency (see Fig. 10b). The Table 4 represents these characteristics of the thruster at 2000 RPM.

In fact, as the advance ratio increases, the thrust coefficient curve of the thruster tends to decrease; in contrast, the power coefficient curve is slightly increased at J in the
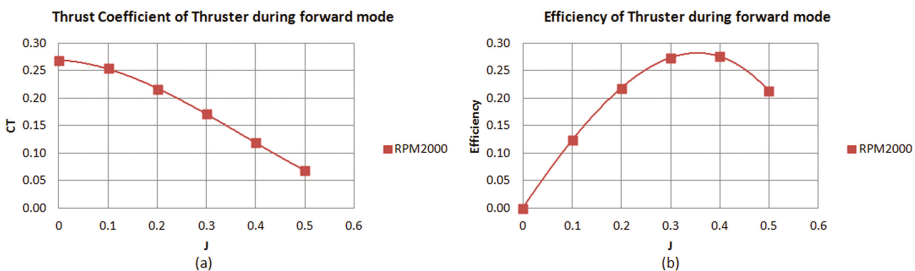

Fig. 10. Thrust coefficient (a), efficiency (b) of thruster during forward mode at 2000 RPM

Table 4. Forward mode performance of the LBV150 ROV thruster at 2000 RPM

J	C_T	C_P	Efficiency
0.1	0.255	0.205	0.124
0.2	0.216	0.199	0.217
0.3	0.171	0.188	0.273
0.4	0.120	0.174	0.276
0.5	0.068	0.160	0.213

range of [0; 0.1], then decreased. The maximum efficiency of the thruster during forward mode is about 28% at J in the range of [0.3; 0.4] which corresponds to the design point of the SeaBotix LBV150 ROV, then it drops dramatically to zero.
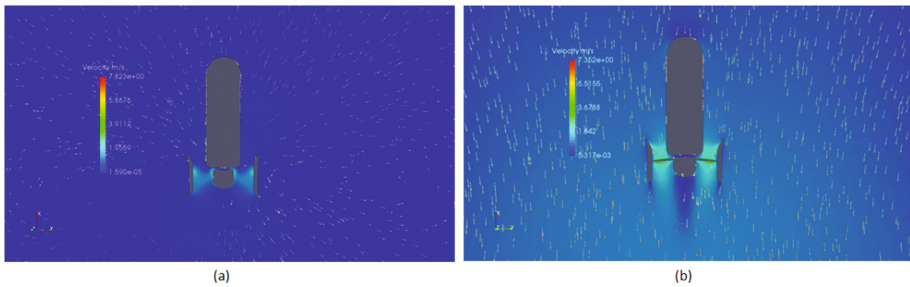

Fig. 11. Flow distribution around the thruster during forward mode (a) at 2000 RPM in static condition; (b) at 2000 RPM with J = 0.4

Figure 11 represents the water flow distribution around the thruster during forward mode at 2000 RPM in static condition and in case of J being equal to 0.4. As can be seen from the figure, in static condition, the water flow, which does not initially move inside the channel, changes the velocity gradient around the thruster. Since the movement of water flow behind the duct is faster than that of the nearby region, the vortexes are generated outside of the duct. In contract, there is no vortex around the duct in case of dynamic flow. This can be explained by the fact that the difference between stream which is accelerated by the propeller and the flow of the channel is smaller compared to that value in static case. Actually, the streamline outside the duct slightly change the direction, and in large scale, the movement of flow outside the duct can be seen as vortex. However, the vortex flow is hindered by the boundary effect.

The simulation results are conducted by using a parallel processing approach. The parallel process runs the public domain openMPI implementation of the standard message passing interface (MPI) by default, although other libraries can be used, using the MPI protocol to send processing information to each chip to calculate. So after a case has been run in parallel, it can be reconstructed for post-processing. Computations are performed using 16 processors (CPU AMD Ryzen 7, RAM 16 Gb). The average processing time for static condition is 8 h to 10 h after approximately 5000 ÷ 7000 iterations. For dynamic condition, the average processing time is 5 h to 6 h after approximately 3000 ÷ 4000 iterations.

5   Conclusions

This article has presented a numerical analysis for prediction of dynamics of the Seabotix LBV150 ROV thruster during forward mode using OpenFOAM. The characteristics of this thruster obtained by the simulation was validated with experimental results obtained by the HCMUT testing system in static cases; and compared with the datasheet of the thruster. These highly accurate results confirm the accuracy of numerical analysis frame, which was deployed in this study and can be applied to investigate the dynamic responds of similar thrusters in other remotely operated underwater vehicles.

References

1. Yoerger, D.R., Bradley, A.M., Jakuba, M., et al.: Autonomous and remotely operated vehicle technology for hydrothermal vent discovery, exploration, and sampling. Oceanography **20**(1), 152–161 (2007). Special issue feature
2. Anderson, J.D.: Computation Fluid Dynamics – The Basic with Applications. McGraw-Hill Education, New York (1995)
3. Wilcox, D.C.: Turbulence Modeling for CFD. DCW Industries, La Cañada Flintridge (2006)
4. Quan, N.N.H., Hieu, N.K., Nha, N.T.: Simulation of the characteristics of the ducted "Master Airscew E9×6" propeller with ANSYS CFX. In: Proceedings of Vietnam National Conference on Fluid Mechanics, Ha Noi (2016)
5. Quan, N.N.H., Hieu, N.K.: Numerical simulation of the 3-seater hovercraft's ducted propeller performance. In: 11th SEATUC Symposium, Ho Chi Minh, Vietnam (2017)
6. Thien, P.Q., Hieu, N.K.: On modeling of a small UAV's propeller for CFD simulation in low Reynolds numbers. Sci. Technol. Dev. **18**(K8) (2015)
7. He, X., Zhao, H., Chen, X., Luo, Z., Miao, Y.: Hydrodynamic performance analysis of the ducted propeller based on the combination of multi-block hybrid mesh and Reynolds stress model. J. Flow Control Measur. Vis. **3**, 67–74 (2015)
8. BTD150 AUV/ROV Thruster – Powerful small robust thruster, Teledyne Seabotix BTD150 Datasheet (2015)
9. https://openfoam.org/
10. Morgut, M., Nobile, E.: Comparison of hexa-structured and hybrid-unstructured meshing approaches for numerical prediction of the flow around marine propellers. In: 1st International Symposium on Marine Propulsors, Trondheim, Norway (2009)
11. Wilhelm, D.: Rotating flow simulations with Open-FOAM. Int. J. Aeronaut. Aerosp. Res. **S1** (001), 1–7 (2015)
12. Baker, T.: Mesh generation for the computation of flowfields over complex aerodynamic shapes. Comput. Math. Appl. **24**(5–6), 103–127 (1992)
13. Häusler, A.J.: Mission planning for multiple cooperative robotic vehicles. Ph.D. Thesis in Dynamical Systems and Ocean Robotics Lab, Lisboa, Portugal (2015)